Computers & Industrial Engineering 162 (2021) 107749

Contents lists available at ScienceDirect

Computers & Industrial Engineering

journal homepage: www.elsevier.com/locate/caie

Research on adaptive transmission and controls of COVID-19 on the basis of a complex network

Fengjiao Chang [a], Feng Wu [a,b,*], Fengtian Chang [c,d], Hongyu Hou [a]

[a] Department of Industrial Engineering, School of Management, Xi'an Jiaotong University, Xi'an, Shaanxi 710049, China
[b] Key Laboratory of Process Control & Efficiency Engineering (Xi'an Jiaotong University), Ministry of Education, Xi'an, Shaanxi 710049, China
[c] School of Mechanical Engineering, Xi'an Jiaotong University, Xi'an, Shaanxi 710049, China
[d] Department of Manufacturing Automation, School of Construction Machinery, Chang'an University, Xi'an, Shaanxi 710064, China

ARTICLE INFO

Keywords:
COVID-19
Complex network
Transmission dynamics
Adaptive network transmission model
Control measures

ABSTRACT

COVID-19 has caused massive disruption on the global economy and presents a considerable risk to human lives. Some countries have successfully controlled the pandemic by adopting strict measures, such as lockdown and travel restriction, but such methods are difficult to be applied widely due to their huge costs. To explore available and low-cost solutions, this study proposes an adaptive transmission model on the basis of a complex network, and gives control simulation method of COVID-19. The suggested model considers adaptive changes such as travel network and people's travel intention to form a three-level adaptive network transmission model among cities, communities, and people. The improved susceptible–exposed–infectious–recovered–dead transmission process is integrated into the network. Simulation experiments under high-, low-, and conventional-cost controls are performed. In these experiments, the travel restriction and closing cities are considered, and sensitivity analyses of the parameters are conducted to explore low-cost measures. Meanwhile, time duration and application conditions of different controls are discussed. Results show that lockdown is the most effective way, and the contact and infection rates are the two most important factors to control the pandemic. Low-cost combined control measures are feasible and effective for most countries. Finally, several suggestions are given for national and urban preventions and controls of COVID-19 and other infectious diseases in the future.

1. Introduction

Infectious diseases are highly contagious and epidemic. The outbreaks of infectious diseases, such as smallpox in Chinese history, SARS, Ebola, and bird flu, have caused irreversible damage to humans. Currently, human medical capabilities have been greatly improved, but preventing the transmission of infectious diseases remains difficult because of the global village, convenient transportation, and increasing human mobility. In this social situation, the novel coronavirus had a massive outbreak.

The COVID-19 outbreak occurred in Wuhan in December 2019 and was transmitted rapidly to other Chinese cities in a few months. Subsequently, more infected cases were confirmed globally. By January 20, 2021, the World Health Organization (WHO) classified the novel coronavirus as a "public health emergency of international concern." On March 11, the WHO declared the pandemic. The outbreak has led to more than 4,811,000 deaths globally thus far. At the worst stage of COVID-19, the supply chains between countries broke down, numerous large and small companies went bankrupt, and several individuals faced challenges due to unemployment (Verity et al., 2020). To date, more than 235 million patients have been diagnosed around the world, and the numbers are still increasing (Dong et al., 2020). These numbers reveal the great difficulties for controlling a pandemic in various countries, and COVID-19 would not disappear in a short time (Kissler et al., 2020).

Compared with the traditional infectious diseases, COVID-19 has longer latent periods and a stronger camouflage power (Guan et al., 2020). COVID-19 could transmit rapidly to other contact populations by air unnoticed (Chan et al., 2020), a feature which led to its rapid global outbreak, instead of being confined to one country or one city because of global travelling. Contact accelerates the replication of COVID-19 among close-distance populations, and the travelling urges the shifts of COVID-19 among far-distance areas, cities, or even countries. Thus, contact and travelling are the essential factors that induce COVID-19 transmission. Along with the contagion of panic from the infected high-risk places, the induced or mandatory minimal contact and

* Corresponding author at: 28 West Xianning Road, School of Management, Xi'an Jiaotong University, Xi'an, Shaanxi 710049, China.
E-mail address: fengwu830@126.com (F. Wu).

https://doi.org/10.1016/j.cie.2021.107749
Received 10 May 2021; Received in revised form 9 October 2021; Accepted 12 October 2021
Available online 19 October 2021

Nomenclature

v_i^1, v_i^2, v_i^3	city node, community node, and individual people node
$w_{ij}^1, w_{ij}^2, w_{ij}^3$	adaptive network weight between cities, communities, and people
r_j^1, r_j^2	sensitivity coefficient of trains or people to the severity of COVID-19 in city v_j^1 and community v_j^2
s_j^1, s_j^2	confirmed COVID-19 cases in city v_j^1 and community v_j^2
$cw_{m^{(i)}\cdot}$	travelling willingness of all people from community $m^{(i)}$ of city v_i^1 to other cities
$Mcw_{m^{(i)}\cdot}$	maximum proportion of people for normal travel without COVID-19 from community $m^{(i)}$ of city v_i^1 to other cities
g_i^1, g_i^2	impact coefficient of COVID-19 of city v_i^1 on the travelling willingness of local city dwellers and community.
$cN_{m^{(i)}}, cN_{ij}$	number of passengers from community $m^{(i)}$ or city v_i^1 to city v_j^1
$global(\cdot)$	total population of the community
$mw_{i\cdot}$	travelling willingness of all people from community v_i^2 to other local communities in the same city
$Mmw_{i\cdot}$	maximum proportion of people for normal travel without COVID-19 from community v_i^2 to other local communities
mN_{ij}	number of travelers from community v_i^2 to local community v_j^2
q	isolation ratio of susceptible persons
c	contact rate
β	contact propagation probability
σ	transfer rate from latent into infected persons
ρ	probability of symptoms of infected persons
λ	transfer rate from isolated susceptible persons into free susceptible persons
α_I, α_H	mortality ratio of symptomatic infected persons and quarantined infected persons
δ_I, δ_A	isolation ratio of symptomatic and asymptomatic infected persons
δ_q	transfer rate from quarantined latent persons into quarantined infected persons
$\gamma_I, \gamma_A, \gamma_H$	recovery ratio of symptomatic infected persons, asymptomatic infected persons, and quarantined infected persons

travelling in these places lead to dynamic differentiated transmission relative to other places (Bi et al., 2019). The mandatory lockdowns in all communities or high-risk places are feasible and effective measures to control COVID-19. However, this measure is not the most effective one for all countries, such as the United States, because of the high costs for government and the great impact on people. Therefore, further research on the transmission of COVID-19 from contacts and travelling is necessary, along with the exploration of other feasible, effective, and low-cost controlling measures.

Fortunately, a complex network is a promising approach for dealing with the above problems. Nodes could represent people, communities, cities, or countries, whereas edges could reveal existing contacts and travelling. The network could be used to simulate the dynamic transmission of viruses with edges from one person to another or from one place to another. Dynamic transmission models, such as the SI, SIRS, SIS, and SEIR (Kang et al., 2015), could also be constructed with a complex network. However, existing models consider only the static deterministic network and their transmission and ignore dynamic changes in differentiated transmission abilities from various nodes. An adaptive dynamic network transmission model is infrequently employed. Meanwhile, complex networks are still insufficiently researched for revealing the transmission characteristic of COVID-19 and feasible control measures. Thus, to further explore the adaptive transmission and control methods of COVID-19 from a complex network, this work proposes a three-level adaptive network transmission model among cities, communities, and people. This network is combined with comprehensive control simulation measures from the aspect of country.

The remainder of this paper is organized as follows. Section 2 reviews the relevant literature. Section 3 describes the three-level adaptive network transmission model based on a complex network. Section 4 presents the simulation with the collected COVID-19 data in China. Section 5 discusses the COVID-19 transmission under various control scenarios. Finally, the concluding remarks are drawn in Section 6.

2. Literature review

Considering the dynamic and complex transmission characteristics of the novel coronavirus, this section presents research based on complex network theory and the transmission dynamics model on infectious diseases. Then, studies on the transmission and control of COVID-19 are reviewed on the basis of this theory and the correlation models.

2.1. Complex network theory

A network involves sets of nodes and edges and could be classified as a random, regular, or complex network. Complex networks are widely used to investigate node characteristics and their interaction relations (Ahluwalia and Li, 2011). A complex network has one or all properties of self-organization, self-similarity, attractor, small world, and scale-free (Lahrouz et al., 2020). Network research covers physics, biology, technology, society, and other subjects (Chang et al., 2018). In terms of epidemiology, scholars usually considered epidemic transmission in a homogeneous network. In this network, the population is usually assumed to be evenly mixed and all people as equally likely to be infected (Zhu et al., 2012), thereby simplifying network modeling. However, people are heterogeneous, and their social network and travels could substantially affect the spread of infectious diseases. Zhang et al. (2020) demonstrated the correlation between international human movement and outbreaks in priority countries with the global COVID-19 pandemic network. Their work confirmed that a network can influence the transmission for infectious diseases. Weeden and Cornwell (2020) investigated small-world networks to reveal the characteristics of epidemic transmission. Zhu et al. (2015) explored the application of a scale-free network for an epidemic transmission. Marquioni and de Aguiar (2020) and Wang and Peng (2020) presented extensive research. Therefore, the study of infectious disease transmission with a complex network is an important topic.

2.2. Transmission dynamics model

In previous studies, mathematical epidemiology such as compartment model was an important method to describe the transmission of infectious diseases and predict their trends (Okhuese, 2020). In 1926, Kermack and Mckendrick presented the famed susceptible–infectious–recovered (SIR) compartment model (Wang and Peng, 2020) followed by the susceptible–infectious–susceptible (SIS) counterpart. These two classical models used differential equations to simulate the spread of infectious diseases and laid a solid foundation for further transmission dynamics. Subsequently, some extended transmission dynamics models were developed according to the transmission process and different characteristics of infectious diseases. For example, Arenas et al. (2016) used the SI and SIR models to describe the spread of infectious diseases. Li et al. (2014) constructed the SIRS epidemic model to examine the spread of

infectious diseases in complex heterogeneous networks. Denphedtnong et al. (2013) established and analyzed the epidemic susceptible–exposed–infectious–recovered–susceptible (SEIRS) model in two cities. These models play important roles in revealing the changes in infection rates and the trends for infectious diseases. However, appropriate transmission mechanisms warrant further exploration because of the asymptomatic, susceptible, and latent characteristics of COVID-19.

2.3. Transmission and control of COVID-19

Numerous scholars have combined a complex network and a transmission dynamic model to understand COVID-19. Read et al. (2020) used a deterministic SEIR transmission model to estimate the basic reproductive number of COVID-19 and illustrated its transmission severity. Tang, Wang, et al. (2020) presented the SEIR transmission model for COVID-19 in Wuhan to estimate the possible duration of transmission and analyze the impact of traffic restrictions on confirmed cases. Furthermore, Tang, Bragazzi, et al. (2020) utilized reported data to present a dynamics transmission model for predicting the epidemic in China in a short time. Zeng et al. (2020) proposed three model-free methods and a multi-model ordinary differential equation called SEIRSD with a neural network to predict COVID-19 transmission in mainland China. Giordano et al. (2020) proposed the susceptible–infected–diagnosed–ailing–recognized–threatened–healed–extinct (SIDRATHE) model to predict the COVID-19 epidemic in Italy. In terms of epidemic control, with exploratory modelling and analysis, Paul and Venkateswaran (2020) proposed an integrated supply chain-epidemic model to elucidate the epidemic control mechanisms under deep uncertainty. Considering the characteristics of human movement and the advantage of a complex network, Hellewell et al. (2020) structured a branching process model about COVID-19 and discovered that effective contact tracing and case isolation could control the epidemic. Prem et al. (2020) explored the impacts of physical distance and contact on COVID-19 transmission and predicted the resumption of work and production time by employing the SEIR model. Wang et al. (2020) established a complex network model of COVID-19 transmission in Wuhan and 15 surrounding cities on the basis of a human mobility network to explore the impact of work resumption on the epidemic. These studies mostly utilized local networks and rarely considered networks from different levels, such as communities, cities, and countries. Meanwhile, the transmission network dynamically changes with disease severity and travelling. However, the adaptive characteristics of the network are usually ignored or simplified, and this approach is inadequate to reveal the transmission mechanisms of COVID-19.

On basis of the above reviews, we found that research on COVID-19 transmission under a complex network remains insufficient. Adaptive changes of the model are also rarely involved in existing researches. Therefore, to extend the literature and develop low-cost containment for similar infections, this study proposes an adaptive transmission model based on a complex network involving population mobility, social structure, and infectious disease transmission. In addition, adaptive transmissions for COVID-19 in mainland China under three scenarios of high-, low-, and conventional-cost controls are simulated and discussed. The proposed modeling methods and low-cost combined controlling measures are verified to be feasible and effective for curtailing nationwide COVID-19 or similar infections.

3. Adaptive COVID-19 transmission model based on a complex network

A three-level adaptive network transmission model framework for COVID 19 is firstly presented to simulate the nationwide transmission. The framework includes the personnel travel network model between cities and between communities and the population contact network model between people. These models are built respectively from an adaptive intercity travel network, an intercommunity travel network and a population contact network, and their network transmission process for the novel coronavirus.

3.1. Adaptive network transmission model framework of COVID-19

Learning from the propagation characteristic of COVID-19, we assume that the coronavirus is transmitted along with the movement and contact of people. The contact leads to the replication of the coronavirus from one person to another, whereas the movement causes the shift of the coronavirus from one place to another. Movement is classified into community and city travel according to the distance. Thus, the proposed model includes three sub-models: personnel travel network model between cities (I-level), personnel travel network model between communities (II-level), and population contact network model between people (III-level) (Fig. 1).

In I-level, we take all Chinese cities with train stations as nodes. They are interconnected by intercity travel networks based on the rail passenger network. The coronavirus is transmitted from one city to another through infected passengers. In II-level, the inner communities in each city are deemed as nodes interconnected by the constructed intercommunity travel network based on a BA scale-free complex network similar to the road traffic. The coronavirus is transmitted from one community to another through infected travelers. In III-level, the individuals in each community are regarded as nodes that are interconnected by the built population contact network based on the fully connected complex network. The susceptible–exposed–infectious–recovered–dead (SEIRD) transmission model is applied to reveal the probabilistic dynamic transmission process. Each city node in I-level has an intercommunity travel network in II-level, whereas each community node in II-level has a population contact network in III-level. Meanwhile, the travel networks in I-level and II-level could change adaptively and dynamically along with the severity of COVID-19 in the corresponding city or community nodes. The detailed model is introduced in the next section.

3.2. I-level: Personnel travel network model between cities

3.2.1. Intercity travel network

In this paper, the intercity travel network mainly takes train railway as the main ways. Roadways are considered in intercommunity travel, and restricted and fewer waterways and airways will not be concerned. In the railway passenger network, the municipal cities are defined as nodes $v_i^1(i \in (1, N_{city}))$, and the existing railways between v_i^1 and v_j^1 are regarded as the edge e_{ij}^1. The initial weight w_{ij0}^1 of e_{ij}^1 is set as the number of trains passing from city v_i^1 to v_j^1. Thus, the initial intercity travel network is constructed. The edge weights of the network are assumed to change adaptively to reveal the impact of COVID-19 on the personnel travel between cities for business, tourism, or other reasons. This adaptive change depends on the severity of COVID-19 in each city. The higher the severity of the connected city nodes, the fewer the trains between these cities, leading to smaller edge weights. By contrast, nodes with lower severity have weightier edges. Therefore, we set s_j^1 as the confirmed infected cases of COVID-19 in city v_j^1 to reveal the severity. According to s_j^1, the corresponding edge weight w_{ij}^1 would be updated adaptively as

$$w_{ij}^1 = max(w_{ij0}^1 - r_j^1 s_j^1, 0) \quad (1)$$

where w_{ij}^1 represents the dynamic number of trains passing from city v_i^1 to v_j^1 during COVID-19, w_{ij0}^1 stands for the initial number of trains without COVID-19, and r_j^1 is the sensitivity coefficient of trains to the severity of COVID-19. The higher the severity and confirmed infected cases of COVID-19, the lower the travelling willingness of people, leading to fewer trains.

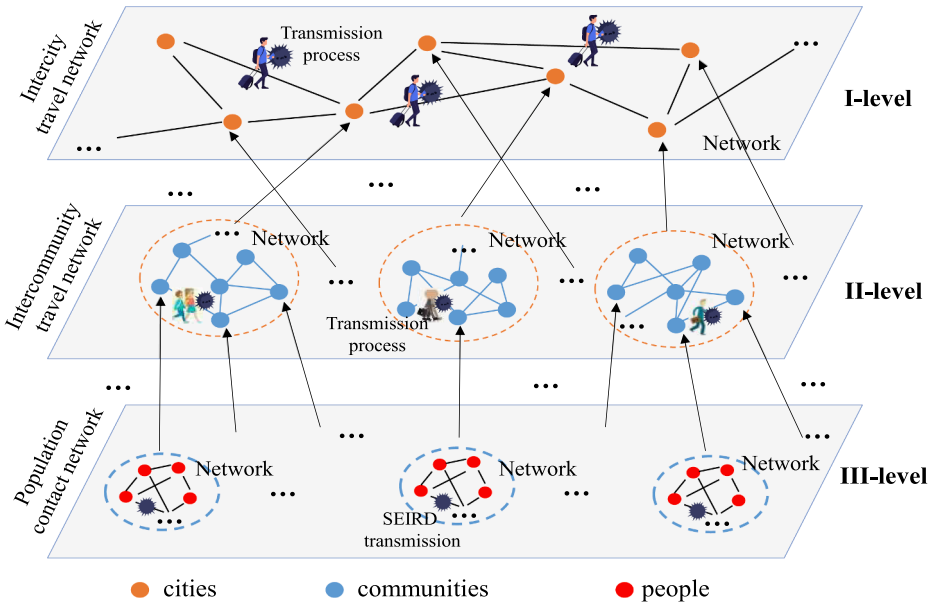

Fig. 1. Framework of the three-level adaptive network transmission model.

3.2.2. Network transmission process

On the basis of the above intercity travel network, the travel processes of passengers are formulated to reveal the network transmission processes of the coronavirus between cities. Simulating everyone's travel process is challenging. Therefore, we calculate the number cN_{ij} of passengers from one city to another under travel willingness $cw_{m^{(i)}.}$ and travel probability p_{ij}^1. The higher the number of passengers, the higher the probability the coronavirus is transmitted between cities. The detailed formulation is displayed as follows:

$$p_{ij}^1 = w_{ij}^1 \Big/ \sum_{k \in V_{i.}^1} w_{ik}^1 \tag{2}$$

$$cw_{m^{(i)}.} = max(Mcw_{m^{(i)}.} - g_i^1 s_i^1,\ 0)\ m^{(i)} \in (1, N_{com}^{(i)}) \tag{3}$$

$$cN_{m^{(i)}} = cw_{m^{(i)}.} \times global(m^{(i)}) \tag{4}$$

$$cN_{ij} = (\sum_{m=1}^{N_{com}^{(i)}} cN_{m^{(i)}j}) \times p_{ij}^1 \tag{5}$$

where p_{ij}^1 represents the travelling probability of people with trains from city v_i^1 to v_j^1, $V_{i.}^1$ is the node set to which node v_i^1 is connected, $N_{com}^{(i)}$ is the number of communities in city v_i^1, and $cw_{m^{(i)}.}$ is the travelling willingness that is represented by the proportion of intercity travelers relative to the total population.

In the above equations, the number of passengers between cities is defined from the travelling willingness of all the communities of each city and the travelling probability of people with the existing number of trains. In Eq. (2), the adaptive travelling probability is given and is related to the adaptive weights of the intercity travel network. Eq. (3) calculates the travelling willingness from each community where the willingness is affected from the local confirmed infected cases and the impact of COVID-19 on local people. The more cases and higher impact a community has, the lower is its travelling willingness. All the passengers that travel to the same destination cities are assumed to be random and distributed evenly among all the administered communities.

3.3. II-level: Personnel travel network model between communities

3.3.1. Intercommunity travel network

In each city, people usually move to schools, enterprises, factories, downtown, or other places for work, study, and daily life. These places and areas usually have higher concentrations of people than other locations. Thus, movement from one area to another outlines the scale-free network characteristic. Of all ways of transport, road transport is usually associated with travels within city. However, due to the complexity of the road connectivity, it is difficult to achieve restrictions on road traffic. Thus, in this context, the intercommunity travel network is considered to simulate the road traffic and is built according to the BA scale-free network.

Assuming that the population in each city is randomly divided into N_{com} communities, all communities are deemed as a network node $v_i^2 (i \in (1, N_{com}))$. The typical growth and preferential attachment mechanisms from the BA network and random distance weights are introduced to ascertain the network edge e_{ij}^2 and weight w_{ij}^2 from all the nodes.

(1) **Growth:** Initially, we create a fully connected network with small initial m_0 nodes. At each time step t, only one new node is generated and connected to the existing nodes in the network. The growth ends when the total number of nodes reaches N_{com}.

(2) **Preferential attachment:** During the growth, the connection probability that each new node is connected to an existing node is proportional to the degree distribution of the connected node. At each time step t, if the random value is larger than the connection probability, then the connection is created. All the connections could be created for the new node until all existing nodes are evaluated.

(3) **Distance weight determination:** Aiming at the w_{ij}^2 of e_{ij}^2, a 2D rectangular region with a unit side length is first given. All the N_{com} nodes are randomly assigned an unduplicated coordinate (x, y) $(x \in (0,1), y \in (0,1))$ on the plane. Thus, the distance d_{ij}^2 from the community node v_i^2 to v_j^2 could be calculated as $d_{ij}^2 = \sqrt{(y_j - y_i)^2 + (x_j - x_i)^2}$. w_{ij}^2 is the reciprocal of the distance as $w_{ij}^2 = 1/d_{ij}^2$. Thus, the larger the distance, the lower the weight and the transmission probability of the coronavirus between communities.

The initial intercommunity travel network could be built according to the above modeling mechanisms. Similar to those of the intercity travel network, the edge weights of this intercommunity travel network could also be changed to adapt to the severity of COVID-19 in the connected community nodes. Thus, assuming that s_i^2 is the confirmed infected cases in community v_i^1, the weights could be updated adaptively as follows:

$$w_{ij}^2 = max(w_{ij0}^2 - r_j^2 s_j^2, 0) \tag{6}$$

where w_{ij}^2 is the dynamic distance weight from community v_i^2 to v_j^2, and w_{ij0}^2 is the initial random distance weight.

3.3.2. Network transmission process

Similarly, on the basis of the above intercommunity travel network, the travel processes of students, workers, consumers, and other travelers between communities could lead to the transmission of the coronavirus. Therefore, the transmission process in each city could also be defined under the willingness $mw_{i\cdot}$ and travel probability p_{ij}^2 of people from their communities as follows:

$$p_{ij}^2 = w_{ij}^2 \Big/ \sum_{k \in V_{i\cdot}^2} w_{ik}^2 \tag{7}$$

$$mw_{i\cdot} = max(Mmw_{i\cdot} - g_i^2 s_i^2,\ 0) \tag{8}$$

$$mN_{ij} = mw_{i\cdot} \times global(i) \times p_{ij}^2 \tag{9}$$

where p_{ij}^2 represents the travelling probability of people from community v_i^2 to the local community v_j^2, and $V_{i\cdot}^2$ is the set of nodes connected to node v_i^2.

3.4. III-level: Population contact network model between people

3.4.1. Population contact network

In each community, all people could contact each other. This contact is frequent, at close distance, and has high probability. Thus, the population contact network in each community could be built as a fully connected complex network. Individuals are deemed as nodes, and fully connected contact relationships are regarded as edges. In this network, the transmission of the coronavirus between individuals follows the probabilistic transmission dynamic model SEIRD.

3.4.2. SEIRD transmission model

By learning from the SEID model (Tang, Wang, et al., 2020), the novel SEIRD is constructed to reflect the transmission of COVID-19 between people from a community instead of the entire population. This model involves six basic categories, namely, *S* (susceptible), *E* (exposed), *I* (infected), *A* (asymptomatic), *R* (recovered), and *D* (dead), and four additional categories, namely, *Aq* (quarantined asymptomatic infected), *Sq* (quarantined susceptible), *Eq* (quarantined latent), and *H* (quarantined confirmed infected). The SEIRD model extends the ignored isolation impacts from asymptomatic, susceptible, latent, and confirmed patients as well as their conversion relations. *R* and *D* are also introduced.

The model is simplified by giving the following assumptions:

1) All individuals in one community have the same infection risk.
2) Antibodies will be produced after the infected persons recover. This assumption indicates that persons from *R* will not be re-infected.
3) The infected, latent, and asymptomatic persons have different abilities to infect susceptible persons *S* and thus to make them become the latent persons *E*.

According to these assumptions, the conversion relations among *S*, *E*, *I*, *A*, *R*, *D*, *Aq*, *Sq*, *Eq*, and *H* are displayed in Fig. 2.

The detailed SEIRD transmission dynamic model is constructed as follows:

$$\frac{dS}{dt} = -[c\beta + cq(1-\beta)]S(I + A + \theta E) + \lambda S_q \tag{10}$$

$$\frac{dE}{dt} = c\beta(1-q)S(I + A + \theta E) - \sigma E \tag{11}$$

$$\frac{dI}{dt} = \sigma\rho E - (\delta_I + \alpha_I + \gamma_I)I \tag{12}$$

$$\frac{dA}{dt} = \sigma(1-\rho)E - \delta_A A - (1-\delta_A)\gamma_A A \tag{13}$$

$$\frac{dS_q}{dt} = cq(1-\beta)S(I + A + \theta E) - \lambda S_q \tag{14}$$

$$\frac{dE_q}{dt} = c\beta q S(I + A + \theta E) - \delta_q E_q \tag{15}$$

$$\frac{dA_q}{dt} = \delta_A A - \gamma_A A_q \tag{16}$$

$$\frac{dH}{dt} = \delta_1 I + \delta_q E_q - (\alpha_H + \gamma_H)H \tag{17}$$

$$\frac{dR}{dt} = \gamma_I I + \gamma_H H + (1-\delta_A)\gamma_A A + \gamma_A A_q \tag{18}$$

$$\frac{dD}{dt} = \alpha_I I + \alpha_H H \tag{19}$$

In the above equations, each community has a local SEIRD transmission model to reveal the local transmission of the coronavirus. First, susceptible persons could have contact with a latent patient, asymptomatic infected person, or infected person at a probability of *c* and become infected or exposed at the probability of β. Second, with contact tracing, susceptible persons are isolated as *Sq* or *Eq* at the rate of *q*, *Eq* is converted into *H* at the probability of δ_q, and quarantined confirmed infected persons may die or recover. Finally, exposed individuals show symptoms of infection with the proportion ρ, and asymptomatic patients are isolated as *Aq* with probability δ_A and recovered with probability γ_A. Those with symptoms are converted to *H*, *R*, and *D* at the probability of δ_I, γ_I, and α_I, respectively.

Eq. (10) shows that susceptible persons could become exposed or that they are isolated as *Sq* or *Eq*. Eqs. (11)–(13) reveal the transformation of *E*, *I*, and *A*. Eqs. (14)–(16) disclose the changes in *Sq*, *Eq*, and *Aq* under isolation measures. Eqs. (17)–(19) indicate the changes in *H*, *R*, and *D*.

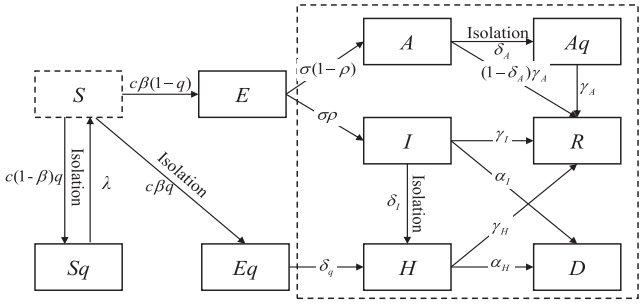

Fig. 2. Local SEIR transmission model and their conversion relations.

4. Simulation of COVID-19 transmission

4.1. Railway network and population data

In this study, railway station information for 321 cities was collected, and the number of trains on January 10, 2020 was used to build the intercity travel network. The network includes 2515 railway stations and 11,111 trains. Population data for all cities across the country were also collected for the personnel travel network. The city population heat map is shown in Fig. 3 to indicate the distribution of cities and their population density.

The intercity transport network flow map according to the collected information is shown in Fig. 4. It contains 321 city nodes, and is built on the city population heat map. The realization point is the starting point of the line segment, and the hollow circle is the end point of the line segment. The larger the flow, the thicker the line. The direction of the traffic is represented by nodes, starting at a solid point and ending at a hollow ring.

4.2. Sample data

A system of daily and zero reporting of pneumonia cases from the novel coronavirus was implemented in China since January 20, 2020. Therefore, we used the epidemic data for each city reported on January 20 as the initial data of the model simulation. That data included the population for each city and the cases of infection, medical observation, suspicion, recovery, and death. In addition, the total epidemic data of COVID-19 in mainland China from January 20 to February 6 were collected, including the existing cases, accumulative cases, accumulative cured population, and accumulative death cases. These data could be used to simulate and estimate the relevant parameters in the model.

4.3. Parameter settings

In this section, some parameters were set to form the spreading model for COVID-19. First, to simplify the intercommunity travel network, we set the number of II-level nodes as 10, 30, 60, 110, and 160 according to the size and type of cities. Second, in terms of people's sensitivity to the epidemic, we set $r_j^1 = r_j^2 = 0.001$, $g_i^1 = 10{,}000$, and $g_i^2 = 50{,}000$ according to the survey from some individuals. Third, the initial state of the population of each community in a city was assumed to follow a standard normal distribution. The total population from all the communities in one city is equal to the collected population data from the city. Finally, simulation experiments were used to estimate other parameters.

4.4. Simulation

The least squares method was used to estimate some parameter values in the SEIRD model by fitting the case data for 17 days after January 20, 2020. The related parameters are listed in Table 1. The fitting curves are shown in Fig. 5. Two indexes were applied, including the symmetric mean absolute percentage error (SMAPE) and the coefficient of determination (R^2), to evaluate the fitting effects (Table 2).

The results indicate that the fitting curves could fit the trends for the four published data with good results, thereby confirming that the parameters obtained by the fitting operation could correctly reflect the national transmission of COVID-19 in the early stage.

On basis of the above parameters, a further simulation prediction experiment was conducted. Fig. 6 shows that the number of confirmed cases nationwide could reach approximately 2.5 million after 60 days when the transmission parameters were unchanged and no travel restrictions were imposed. The simulated curve was higher than the actual reported data because some measures, such as lockdown and traffic limiting, were not considered in this simulation experiment. To examine effective control measures for COVID-19 in complex networks, we analyzed and compared the effects of different intensity control measures to generate effective recommendations for coping with COVID-19 and other similar contagions.

5. Transmission under various control scenarios

In this section, we conducted experiments to predict the overall epidemic trends with three types of controls across the country, including conventional-, high-, and low-cost controls. The cost-saving measures were also explored to curb the epidemic. These analyses used the national epidemic data released on January 20 as the initial state and simulated more than 60 days of transmission, i.e., the experiments entailed 60 iterations.

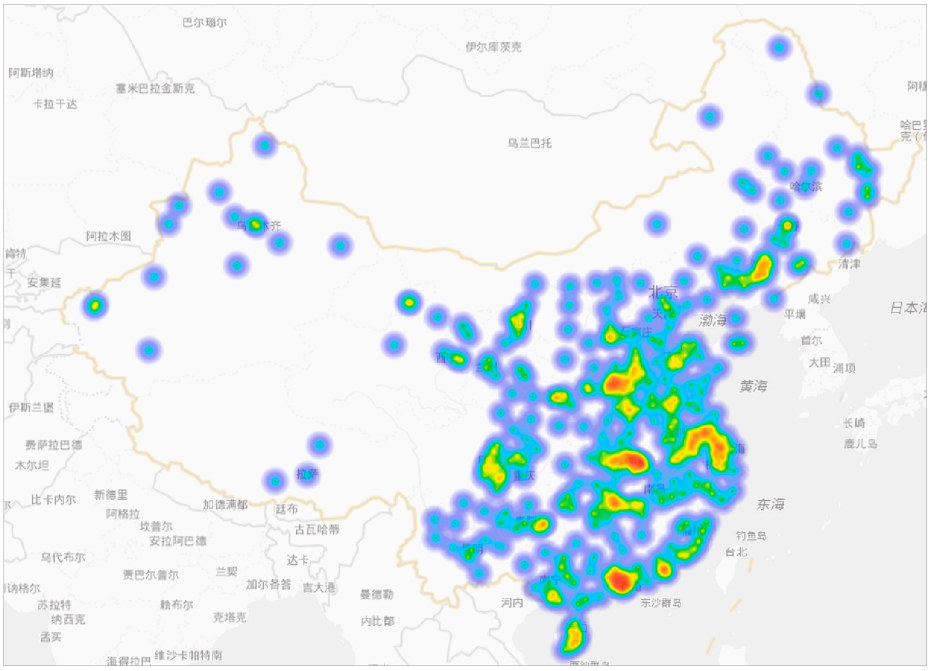

Fig. 3. The city population heat map.

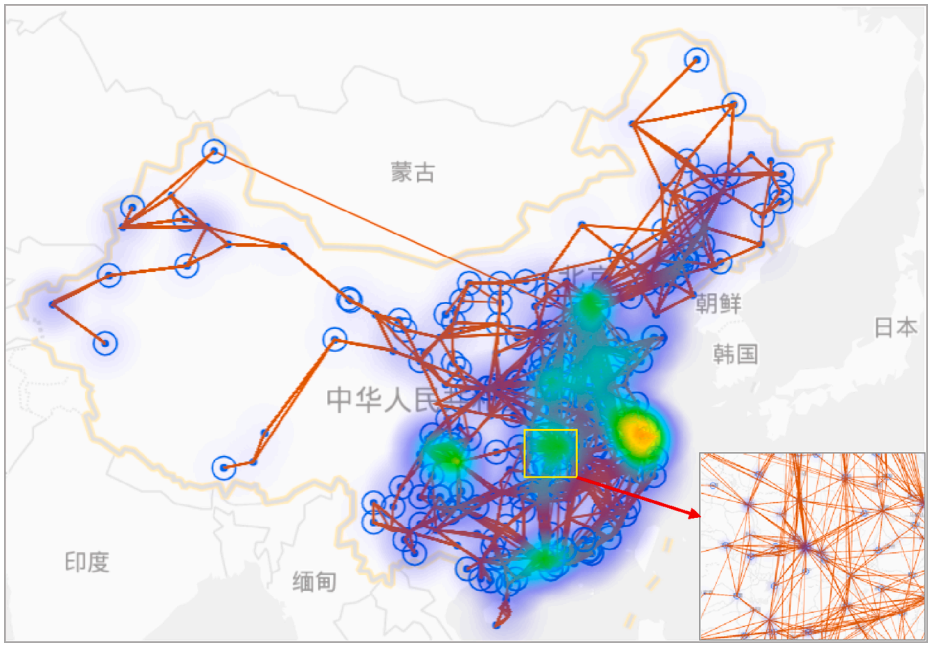

Fig. 4. The intercity transportation network flow map.

Table 1
Estimated parameter values in the SEIRD model.

Parameter	Value	Data Source	Parameter	Value	Data Source
λ	1/14	NHC	σ	1/7	WHO
q	1.2858×10^{-5}	(Tang, Wang, et al., 2020)	ρ	0.86834	(Tang, Wang, et al., 2020)
c	28.781	PE	α_I	0.00582	PE
β	8.54×10^{-8}	PE	α_H	0.00282	PE
γ_I	0.00729	PE	δ_I	0.13266	PE
γ_A	0.00624	PE	δ_A	0.13	PE
γ_H	0.01578	PE	δ_q	0.1259	PE

PE: Parameter Estimation Method; WHO: World Health Organization; NHC: National Health Commission of the People's Republic of China.

5.1. Scenario 1: Conventional controls

In this paper, conventional controls refer to such measures that could have less impact on people's life and enable our work and study to be carried out normally. These controls involve isolation of confirmed cases and contact tracing to quarantine virus transmission. In this scenario, the suspected patients could be quarantined and become parts of *Sq*, *Eq*, or *Aq*; the confirmed patient could be admitted to a hospital; and no other coercive control measures would be taken.

In this experiment, we used the initial parameters obtained in Section 3 to simulate COVID-19 spread across the country under the conventional controls and predict infectious cases. Fig. 7 shows that if control measures remain constant, the cumulative amounts would increase almost linearly after 50 days and the epidemic would not reach an inflection point in a year. The epidemic could even last at least 2 years. Furthermore, the total confirmed number could exceed 60 million. Although classic controls would not affect people's normal lives in the short term, serious national security issues and social panic would arise in the long term. But in the pandemic era, it is essential to implement this control strategies all the time and everywhere.

5.2. Scenario 2: High-cost controls

During this epidemic, the Chinese government responded promptly and actively implemented a series of high-cost and strict prevention and mandatory control measures. The measures include nationwide lockdown and travel restrictions. In a short period of 2 months, the cumulative number of cases essentially stopped growing. Even though the measures were effective, they entailed huge costs. For example, China's tourism, entertainment, catering, and other service industries were hit hard, causing widespread unemployment. To explore the effects of high-cost controls, the experiment assumed to restrict inter-city travel and inter-community travel of the city and set the corresponding network edge weight to 0 if the city was closed. Simultaneously, the contact and infection rates within the communities of this city were reduced, and the recovery rates were improved to fit the actual epidemic prevention and control status in China.

In this experiment, we firstly analyzed the effects from closing severe epidemic cities at different time nodes. Fig. 8(a) and (b) depicts the results of closing Wuhan on days 1, 10, 20, 30, 40, and 50. Clearly, confirmed cases remained high even though Wuhan was sealed off since January 21, and this outcome was caused by two main reasons. On the one hand, a fairly high proportion of latent infections in Wuhan allowed the infectious disease to continue to spread within the community. On the other hand, by January 20, COVID-19 had spread to other cities. If these cities had not taken any effective measures, then the number of infected people would have inevitably shown the same outbreak trend. The above analysis proves that closing only severe epidemic areas would not slow the spread of infection.

Fig. 8(c) and (d) shows the spread of COVID-19 within 60 days under the joint lockdown measures where Wuhan was closed at different time nodes and other cities were blocked a week later. The cumulative and existing confirmed cases varied significantly at the different closure time nodes. However, all increase rates of confirmed cases decreased. The number of cases peaked for a short time. For example, the six existing case curves reached their peaks and cumulative case curves reached their turning points on days 12, 22, 33, 42, 50, and 59 in Fig. 8(d). The total confirmed cases under two types of measures, including the "Wuhan-1st and other-8th" and "Wuhan-10th and other-18th" in Fig. 8 (c), are under 100,000. These results suggest that lockdown could quickly control the spread of COVID-19 and generate the inflection point. In addition, the figure also shows that the duration of lockdown measures varies with the time of taking measures, but high-cost controls should be implemented at least 2 months until the number of new cases stops growing.

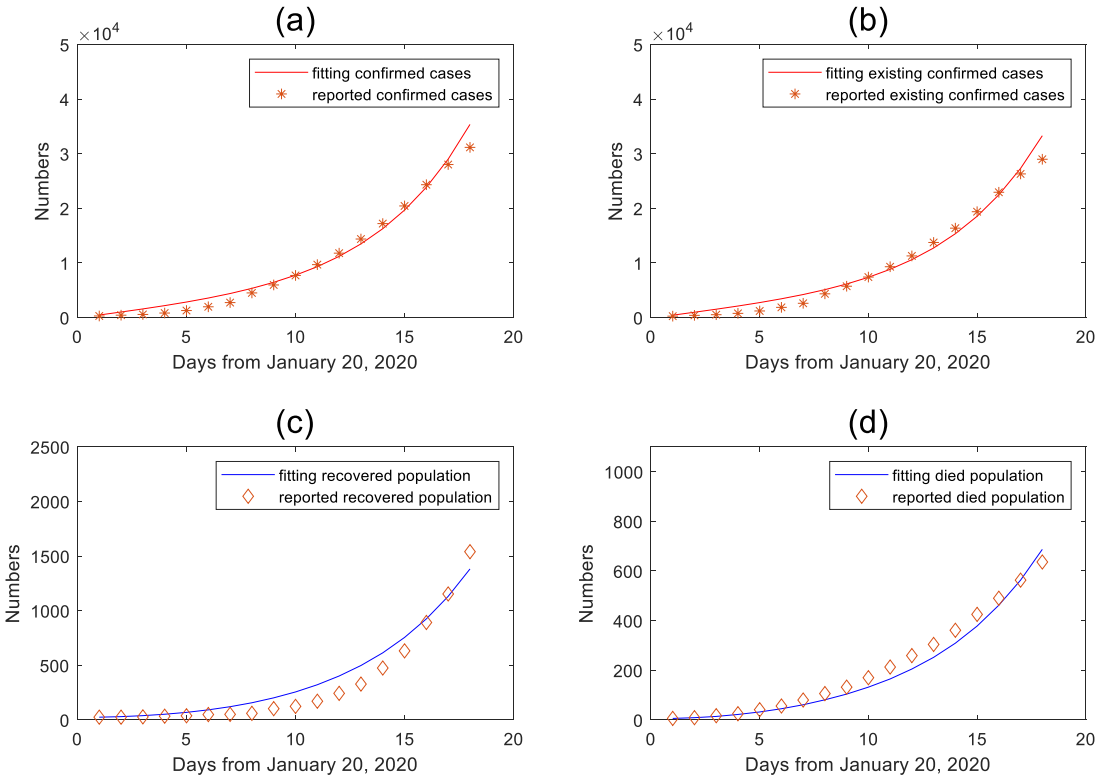

Fig. 5. Fitting curves for (a) existing cases, (b) accumulative cases, (c) accumulative cured population, and (d) accumulative death cases.

Table 2
Error indicators.

Indexes	SMAPE	R^2	Indexes	SMAPE	R^2
Existing	0.000485	0.972453	Recovered	0.006373	0.924064
Cumulative	0.000425	0.975442	Dead	0.002371	0.949104

$SMAPE = (100\%/n)\sum_{t=1}^{n}((|\hat{y}_t - y_t|)/((|y_t| + |\hat{y}_t|)/2))$, $R^2 = 1 - \sum_{i=1}^{n}(y_i - \hat{y}_i)^2 / \sum_{i=1}^{n}(y_i - \bar{y}_i)^2$, where y_t is the actual value, $\hat{y}_t$ is the forecast value, and $\bar{y}_t$ is the average actual values.

The joint lockdown measures have obviously brought the epidemic under control, and the existing cases have gradually declined. In analyzing the causes, we discovered that the joint lockdown not only significantly interrupted people's travels and decreased the virus spreading across the country but also reduced the risk of exposure and even infection among people within the community.

5.3. Scenario 3: Low-cost controls

At present, the global epidemic has not yet reached a turning point, and the confirmed cases in the United States and other countries continue to increase rapidly. Although the high-cost city-closing measures could prevent the spread of COVID-19, some methods are difficult to be implemented in certain countries, such as the United States, because of their high individualism (Huynh, 2020). In this crisis, investigating low-cost epidemic control measures is vital and conducive to fighting the pandemic. Therefore, we carried out the following experiments.

5.3.1. Sensitivity analysis of important parameters

First, sensitivity analyses were conducted on the important parameters in the model to reveal their effects on the epidemic. We selected

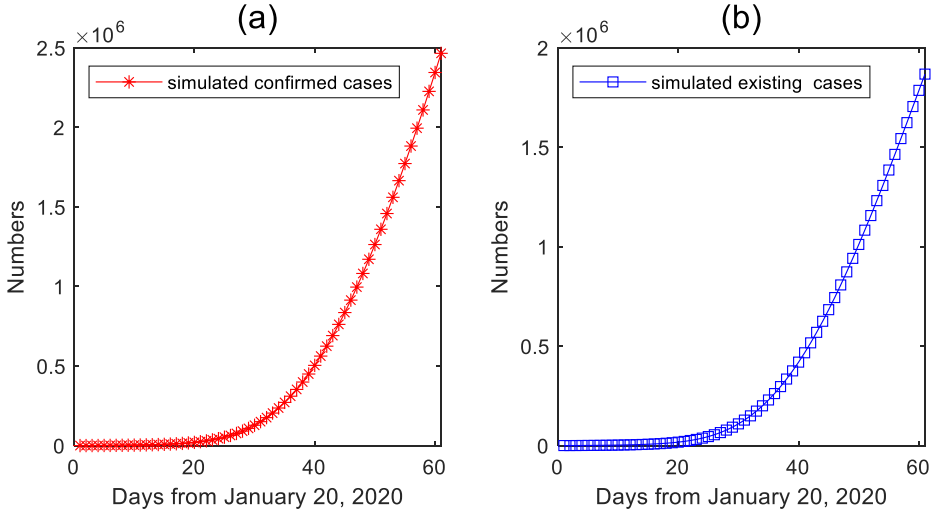

Fig. 6. Confirmed cases without travel restrictions.

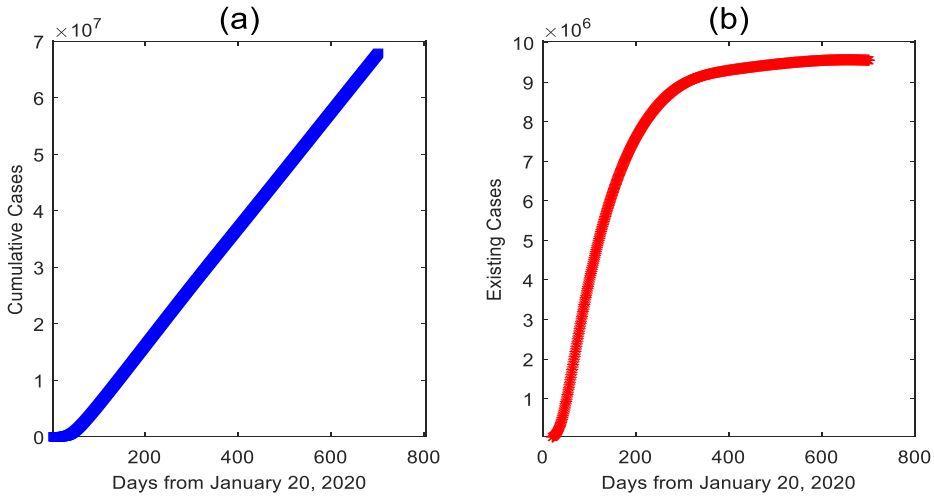

Fig. 7. Change curves of confirmed cases under conventional controls.

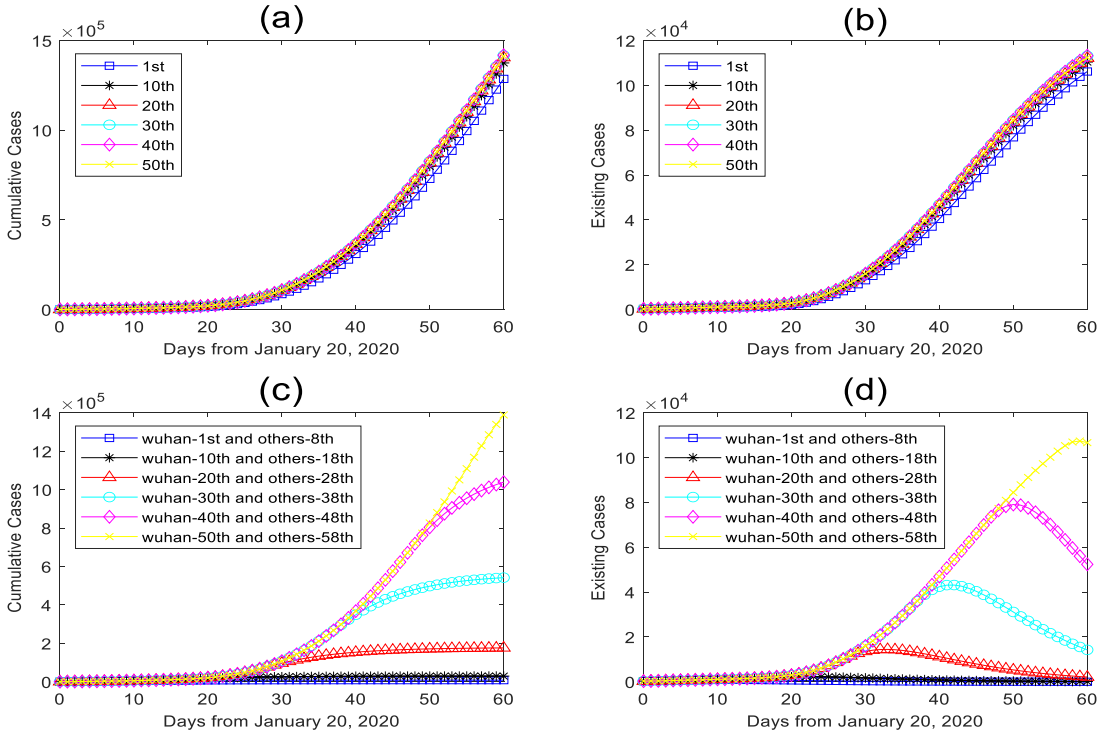

Fig. 8. Change curves of (a and b) cases when blocking Wuhan and (c and d) cases when closing Wuhan and the entire country.

three parameters, namely, contact rates c, infection rates β, and isolation rates q.

As shown in Figs. 9 and 10, when c or β decreases or when q increases, the total confirmed patients at 60 days decrease significantly. However, when q is increased to a certain level, the epidemic could only be controlled by reducing the contact rate c or infection rate β. In addition, as shown in Fig. 9(c) and (d), the transmission of COVID-19 could be curbed when c or β reaches an extremely low level, i.e., one-fifth of the initial values. Thus, the spread of COVID-19 could be curbed by only reducing the infection or contact rates.

Similarly, we investigated how the epidemic might evolve with the different isolation ratios of the asymptomatic δ_A or sensitivity coefficient r. Suppose that r_j^1, r_j^2, g_i^1, and g_i^2 were all increased by the same multiple when r was improved. In this case, Fig. 10(b) and (c) indicate that increasing δ_A or r could only lessen but not stop the spread of infectious diseases, thereby demonstrating that improving public attention to the epidemic could mitigate the transmission of COVID-19 and gain time for the fight against the epidemic.

In summary, the measures that decrease the contact rate c or infection rate β could curb the epidemic, whereas the isolation rate q and sensitivity coefficient r could only reduce and mitigate the transmission of COVID-19.

5.3.2. *Combined measures*

In reality, reducing infection and exposure rates by 80% is difficult. Thus, other combined measures are needed to contain the transmission. Considering the impacts of the parameters on the epidemic and its realizability, we combined four parameters, namely, $0.5c$, 0.5β, $20q$, and $10r$, to ascertain the most efficient low-cost combined measures. The changes in case rates under two-parameter combinations are shown in

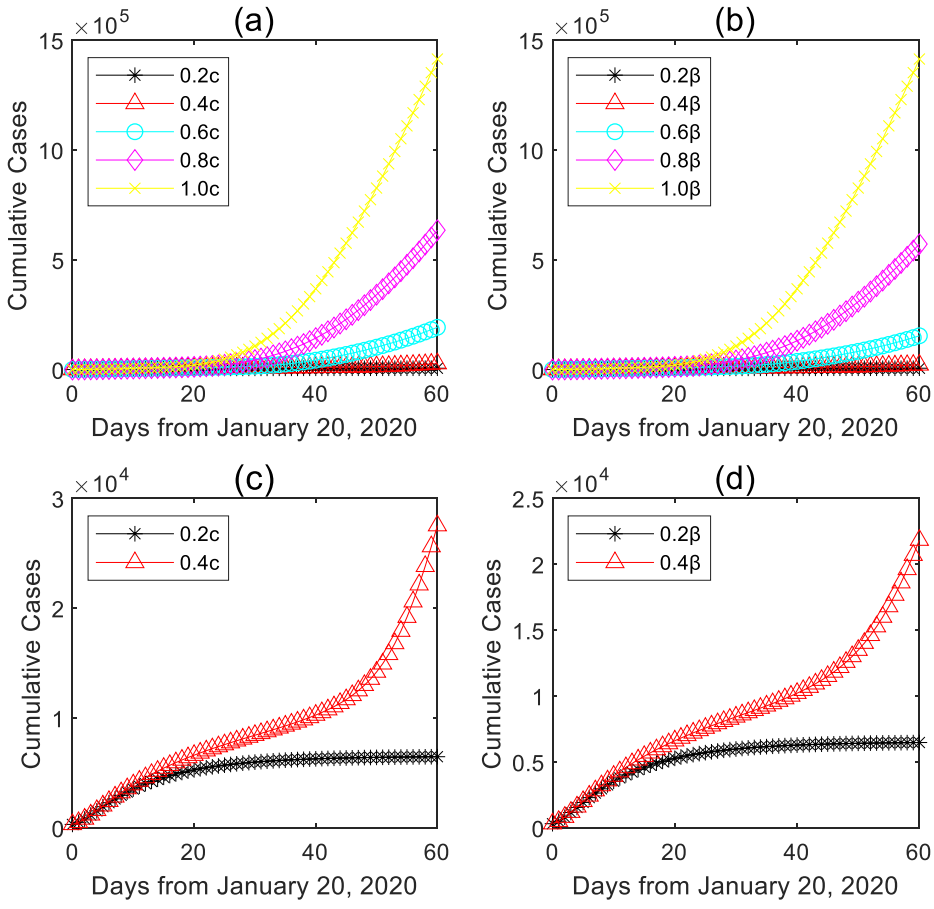

Fig. 9. Accumulative cases at different parameters for the (a, c) contact rate, (b, d) infection rate, and (c) and isolation rate.

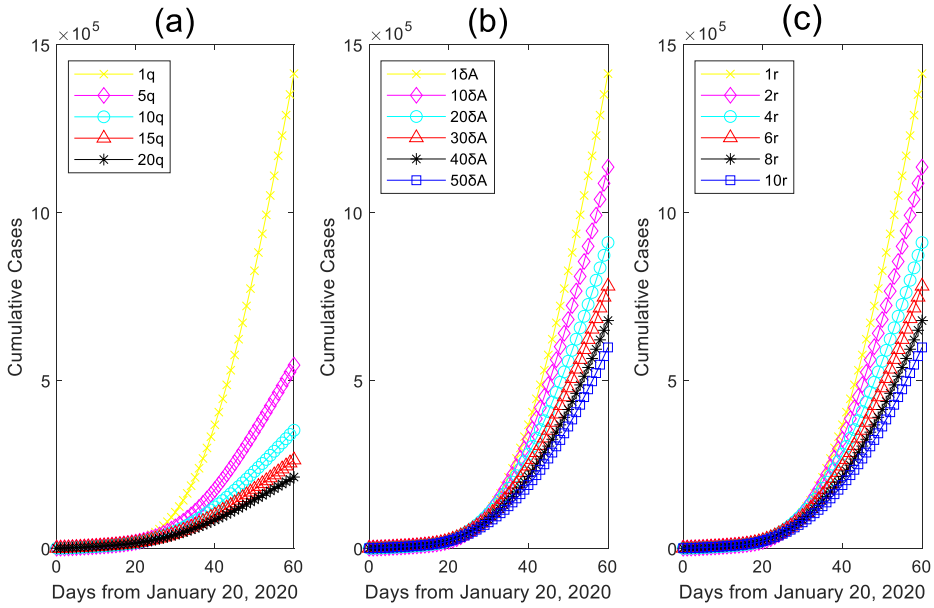

Fig. 10. Accumulative cases at different parameters for the (a) isolation rate, (b) isolation ratio of asymptomatic cases, and (c) people's sensitivity coefficient to the epidemic.

Fig. 11(a) and (c), and the case curves under multiple-parameter combinations are shown in Fig. 11(b) and (d). In these figures, it is only when the contact rate c and infecting rate β are reduced that the turning point will be reached and the infectious diseases will disappear. In addition, when the r and one of c and β are improved, the inflection point of the epidemic will be reached. However, this situation is extremely unstable and can readily cause a second or even multiple outbreaks of the epidemic, such as under the combination of $0.5c$ and $10r$ or 0.5β and $10r$. Finally, in all these combinations, the one that changes c, β, and q concurrently is the most efficient measure.

The three combined parameters are depicted in Fig. 12. Apparently, the last three combinations under the five solutions are all feasible for

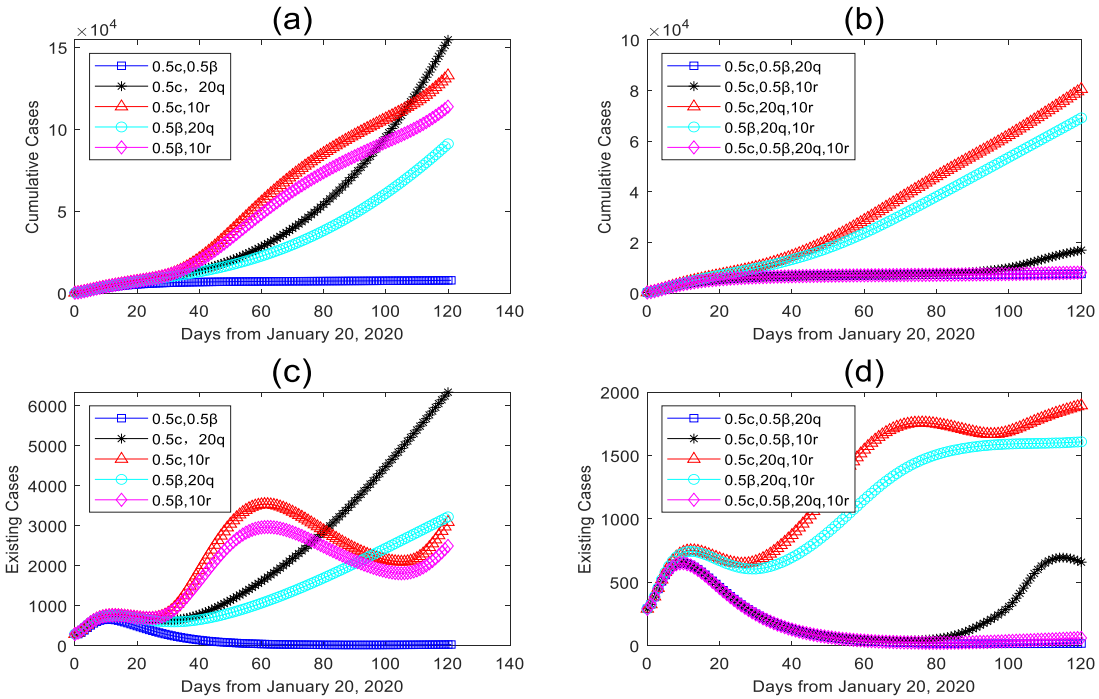

Fig. 11. Change curves of cases under combined measures.

containing the epidemic, namely, (0.5c, 0.5β and 10q), (0.4c, 0.6β and 10q), and (0.6c, 0.4β and 10q). The former two may be easier to achieve. In other words, an optimal outcome would be reached when contact rate c and infecting rate β are at half of their initial values and the isolation rate q is multiplied 10 times. Moreover, from Fig. 12, we find that with this combined measure, the number of existing cases almost falls to a minimum after about 90 days.

5.4. Transmission in other countries

During the pandemic, several western countries also adopted lockdowns for a long time, but the measure was unsatisfactory. For example, on March 10, 2020, nationwide "lockdown" measures were implemented in Italy for approximately a month to avoid the further spread of COVID-19. However, the measure could not stop confirmed cases from increasing significantly, and the epidemic grew out of control.

The transmission model was used to simulate Italy's epidemic. On the basis of Italy's epidemic data on March 10, 2020 and the following 250 days, a fitting process was performed. The fitting curves of confirmed and existing cases are shown in Fig. 13.

Simulation results showed that the Italian contact rate c was 20.8, which is rather higher than the Chinese counterpart of 3.78 during the lockdown. This discrepancy explains why high-cost controls do not exhibit a responsive role in some countries. Therefore, reducing the frequency of human exposure is extremely important to control COVID-19 when a lockdown is implemented.

5.5. Discussion

5.5.1. Conventional and high-cost measures

The above analysis indicates that the epidemic could not be contained and could even last for more than 2 years under conventional controls. This outcome is consistent with the opinion that the epidemic could not end without stringent measures (Lin et al., 2020). However, as

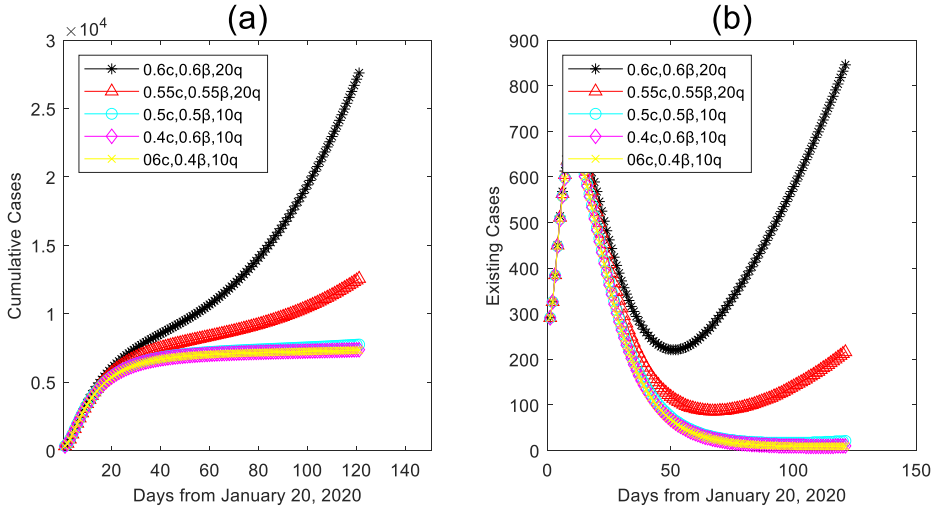

Fig. 12. Change curves of cases under different ratios of parameters.

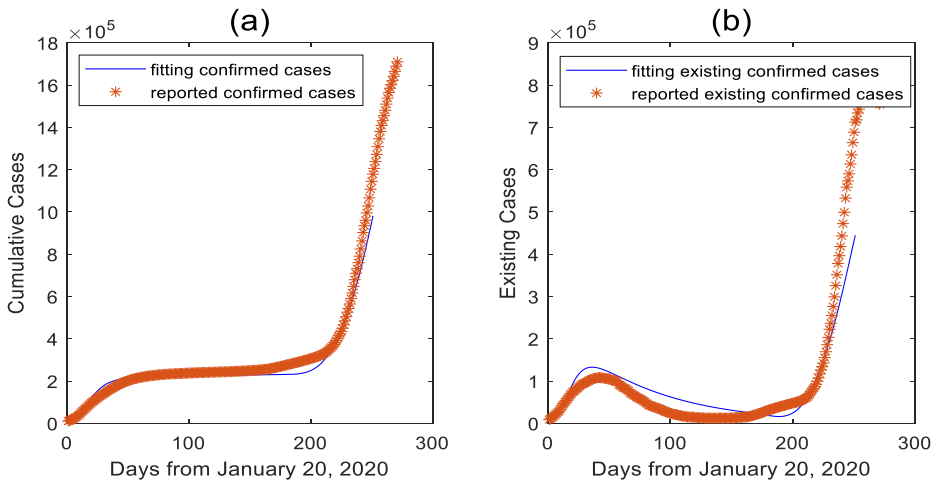

Fig. 13. Simulation curves for Italy.

a routine control measures, conventional measures should be implemented at all times to ensure the effectiveness of the prevention and control mechanism. In addition, high-cost controls in China are undoubtedly the most effective measures to curb the epidemic. In specific, travel restriction and closing cities could contribute to reach the inflection point of the epidemic in just 1–2 months. Therefore, high-cost measures should be implemented for at least 2 months until the number of new cases stops growing. Some countries, such as China and South Korea, have successfully controlled the infection transmission through these measures.

5.5.2. Important parameters

Analyzing the sensitivity of important parameters revealed positive correlations between contact rate c or infection rate β and infected cases. Meanwhile, there were negative correlations between isolation rate q or people's sensitivity to the epidemic r and infected cases. Note that the epidemic would be slowed down with a high enough isolation rate or human sensitivity coefficient and could reach the turning point in a short period if the values of the contact or infection rates were low. Furthermore, in the long run, improving human sensitivity is not advisable because people could become complacent as the situation becomes more optimistic, and this situation is inclined to cause a second outbreak.

In this study, we estimated the average contact and infection rates within communities according to the dataset of the epidemic from January 20 to February 6 in mainland China. The values are higher than other published estimates (Tang, Wang, et al., 2020). In fact, such high contact and infection rates are consistent with the reality that the data were collected during the Chinese New Year and numerous parties and extensive personnel flow occurred at that time. Therefore, reducing those incidences appropriately by implementing strict social distancing and compulsory mask wearing is feasible.

5.5.3. Low-cost combined measures

After analyzing the combined measures, we found that the contact and infection rates are the key factors to contain the transmission and determine if the inflection point could be reached. This conclusion could also be proved in the analysis of high-cost measures, such as closing cities. Moreover, the outbreak would be under control when the contact rate equals $0.5c$ and the infection rate equals 0.5β. That is, within the community, everyone should reduce their contact with others by 50%, and at least half of the people should wear masks to reduce the risk of infection. Besides, this low-cost controls should be carried out for at least 3 months until all existing cases are cured. In brief, we believe that this combined low-cost control is effective and could be achieved through some measures, such as increasing social distancing, compulsory mask wearing, strict contact tracing, and quarantine.

5.5.4. Suggestions

High-cost prevention and control measures must constitute the first choice to control the epidemic in the shortest time. Thus, the lockdown of major cities and the implementation of travel restrictions could contribute to curb the epidemic. Notably, the blockade of a single city has minimal impact on the epidemic. Further restrictions and blockade measures should be taken in most cities and even throughout the country. The earlier the blockade measures are taken, the greater the impact will be on the reduction of the peak number of epidemic infections.

In some countries such as the United States, keeping people at home and preventing them from traveling is difficult because of the local economy and culture. Thus, other low-cost measures could be requisite. When the epidemic is in the outbreak period, increasing the isolation rate can significantly control its development, but the effects are limited. By contrast, reducing the infection and contact rates by 50% could control the epidemic within a controllable range. Therefore, limiting the people flow by 50% and urging more than 50% of people to wear masks to reduce and contain the epidemic in these countries would be vital, even if travel restrictions are not implemented. However, 50% is just a reference criterion under control simulation. It is necessary that all people must wear masks to reduce down the transmission.

More than a year has passed since the outbreak began, and epidemic prevention and control work has become routine in most areas. Thus, sustainable high-cost measures are no longer adapted. At this stage, different areas require different combinations of controls. Therefore, it is necessary to apply the controls from the aspect of country to the city. For example, high-risk areas can adopt local high-cost control measures, but other areas can utilize low-cost combination control measures. Concretely, some cities that exist the clusters of COVID-19 epidemic with multiple simultaneous outbreaks should adopt the high-cost controls, lockdown in the whole city. On the contrary, some cities that have only a few concentrated outbreaks should implement high-cost controls in local areas and the low-cost combination control measures in other most areas. Finally, other cities without outbreaks should implement conventional controls. In the post-epidemic era, flexible combinations of various controls would be indispensable.

6. Conclusions

Contributions of this study include the following

1) A three-level adaptive network transmission model including an intercity travel network, an intercommunity travel network, and a population contact network is presented. The model could adaptively adjust the network transmission along with the dynamic people travel and severity of the epidemic, an outcome that coincides with the actual epidemic situation. Moreover, the novel SEIRD transmission model is constructed and integrated in the population contact network. It covers the isolation from asymptomatic and reveals probabilistic transmission processes of the contact population for COVID-19.
2) The transmission mechanisms of COVID-19 under conventional-, high-, and low-cost controls are simulated, compared, and discussed. High-cost controls are the most effective and immediate measures for the outbreak, but they need strong executive power. The simulation for the Italian epidemic reinforces this view. Low-cost combined measures could also be beneficial for some countries, such as the United States, for which expensive costs are unacceptable and a culture of individualism is emphasized.
3) These controls can also be applied to urban epidemic prevention and control. The high-cost control should be adopted in some cities with clusters and multiple simultaneous outbreaks. In some cities with only a few concentrated outbreaks, the low-cost combination control could be taken in most areas, and the high-cost control in concentrated outbreak areas. Finally, conventional controls should be implemented in other cities without outbreaks.
4) The important key factors to contain COVID-19, such as contact and infection rates, are explored. If the contact and infection rates are both decreased to 50%, the epidemic would be contained in a short time with relatively lower cost. For the contact rate, daily exposure must be reduced by more than 50% (such as limiting mall visits by 50% or decreasing the number of crowd gatherings by 50%). For the infection rate, vaccine development or personal prevention could be valid. For instance, it is encouraged that more than 50%, even all of individuals should wear masks.

Our studies have some limitations. Certain parts of our model are set up to be too simple. For example, the number of trains between cities is assumed to vary linearly with the number of confirmed cases. In fact, the relationship between the epidemic and movement of people between cities or communities is complex and needs to be further defined. Moreover, our work depends on the initial data of the epidemic in China, and this approach is insufficient for some countries for certain reasons, such as culture, economy, and politics. In addition, we assume under high-cost controls, all cities are put under strict lockdown simultaneously. But it is difficult to be carried out in some regions due to the different functionalities of different cities. Therefore, further analyses of the epidemic in other countries and different controls in different cities are required. In the future research, complex and realistic spreading models of infectious diseases should be examined to simulate real complex systems of disease transmission in different countries and cities.

CRediT authorship contribution statement

Fengjiao Chang: Conceptualization, Methodology, Software, Writing – original draft, Data curation. **Feng Wu:** Supervision, Funding acquisition, Project administration, Writing – review & editing. **Fengtian Chang:** Software, Investigation, Data curation, Writing – review & editing. **Hongyu Hou:** Writing – review & editing.

Declaration of Competing Interest

The authors declare that they have no known competing financial interests or personal relationships that could have appeared to influence the work reported in this paper.

Acknowledgement

This work was supported by National Natural Science Foundation of China under grant numbers 71871177 and 71731009.

References

Ahluwalia, R., & Li, C. (2011). An efficient approach to representation and simplification of complex networks. *Computers and Industrial Engineering, 61*(3), 525–528. https://doi.org/10.1016/j.cie.2011.04.007

Arenas, A. J., González-Parra, G., & Chen-Charpentier, B. M. (2016). Construction of nonstandard finite difference schemes for the SI and SIR epidemic models of fractional order. *Mathematics and Computers in Simulation, 121*, 48–63. https://doi.org/10.1016/j.matcom.2015.09.001

Bi, K., Chen, Y., Zhao, S., Ben-Arieh, D., & Wu, C. H. (2019). Modeling learning and forgetting processes with the corresponding impacts on human behaviors in infectious disease epidemics. *Computers and Industrial Engineering, 129*, 563–577. https://doi.org/10.1016/j.cie.2018.04.035

Chan, J. F. W., Yuan, S., Kok, K. H., To, K. K. W., Chu, H., Yang, J., Xing, F., Liu, J., Yip, C. C. Y., Poon, R. W. S., Tsoi, H. W., Lo, S. K. F., Chan, K. H., Poon, V. K. M., Chan, W. M., Ip, J. D., Cai, J. P., Cheng, V. C. C., Chen, H., … Yuen, K. Y. (2020). A familial cluster of pneumonia associated with the 2019 novel coronavirus indicating person-to-person transmission: a study of a family cluster. *The Lancet, 395* (10223), 514–523. https://doi.org/10.1016/S0140-6736(20)30154-9

Chang, F., Zhou, G., Xiao, X., Tian, C., & Zhang, C. (2018). A function availability-based integrated product-service network model for high-end manufacturing equipment. *Computers and Industrial Engineering, 126*, 302–316. https://doi.org/10.1016/j.cie.2018.09.043

Denphedtnong, A., Chinviriyasit, S., & Chinviriyasit, W. (2013). On the dynamics of SEIRS epidemic model with transport-related infection. *Mathematical Biosciences, 245*(2), 188–205. https://doi.org/10.1016/j.mbs.2013.07.001

Dong, E., Du, H., & Gardner, L. (2020). *COVID-19 Dashboard by the Center for Systems Science and Engineering (CSSE) at Johns Hopkins University (JHU)*. Retrieved from https://www.arcgis.com/apps/dashboards/bda7594740fd40299423467b48e9ecf6 Accessed October 5, 2021.

Giordano, G., Blanchini, F., Bruno, R., Colaneri, P., Di Filippo, A., Di Matteo, A., & Colaneri, M. (2020). Modelling the COVID-19 epidemic and implementation of population-wide interventions in Italy. *Nature Medicine, 26*(6), 855–860. https://doi.org/10.1038/s41591-020-0883-7

Guan, W., Ni, Z., Hu, Y., Liang, W., Ou, C., He, J., Liu, L., Shan, H., Lei, C., Hui, D. S. C., Du, B., Li, L., Zeng, G., Yuen, K.-Y., Chen, R., Tang, C., Wang, T., Chen, P., Xiang, J., … Zhong, N. (2020). Clinical characteristics of coronavirus disease 2019 in China. *New England Journal of Medicine, 382*(18), 1708–1720. https://doi.org/10.1056/nejmoa2002032

Hellewell, J., Abbott, S., Gimma, A., Bosse, N. I., Jarvis, C. I., Russell, T. W., Munday, J. D., Kucharski, A. J., Edmunds, W. J., Sun, F., Flasche, S., Quilty, B. J., Davies, N., Liu, Y., Clifford, S., Klepac, P., Jit, M., Diamond, C., Gibbs, H., … Eggo, R. M. (2020). Feasibility of controlling COVID-19 outbreaks by isolation of cases and contacts. *The Lancet Global Health, 8*(4), 488–496. https://doi.org/10.1016/S2214-109X(20)30074-7

Huynh, T. L. D. (2020). Does culture matter social distancing under the COVID-19 pandemic? *Safety Science, 130*, Article 104872. https://doi.org/10.1016/j.ssci.2020.104872

Kang, H., Lou, Y., Chen, G., Chu, S., & Fu, X. (2015). Epidemic spreading and global stability of a new SIS model with delay on heterogeneous networks. *Journal of Biological Systems, 23*(4), 681–719. https://doi.org/10.1142/S0218339015500291

Kissler, S., Tedijanto, C., Lipsitch, M., & Grad, Y. H. (2020). Social distancing strategies for curbing the COVID-19 epidemic. *MedRxiv*. https://doi.org/10.1101/2020.03.22.20041079

Lahrouz, A., Settati, A., Mahjour, H. E., Jarroudi, M. E., & Fatini, M. E. (2020). Global dynamics of an epidemic model with incomplete recovery in a complex network. *Journal of the Franklin Institute, 357*(7), 4414–4436. https://doi.org/10.1016/j.jfranklin.2020.03.010

Li, C. H., Tsai, C. C., & Yang, S. Y. (2014). Analysis of epidemic spreading of an SIRS model in complex heterogeneous networks. *Communications in Nonlinear Science and Numerical Simulation, 19*(4), 1042–1054. https://doi.org/10.1016/j.cnsns.2013.08.033

Lin, J., Huang, W., Wen, M., Li, D., Ma, S., Hua, J., Hu, H., Yin, S., Qian, Y., Chen, P., Zhang, Q., Yuan, N., & Sun, S. (2020). Containing the spread of coronavirus disease 2019 (COVID-19): Meteorological factors and control strategies. *Science of the Total Environment, 744*, Article 140935. https://doi.org/10.1016/j.scitotenv.2020.140935

Marquioni, V. M., & de Aguiar, M. A. M. (2020). Quantifying the effects of quarantine using an IBM SEIR model on scalefree networks. *Chaos, Solitons and Fractals, 138*. https://doi.org/10.1016/j.chaos.2020.109999

Okhuese, V. A. (2020). Mathematical predictions for covid-19 as a global pandemic. *MedRxiv*. https://doi.org/10.1101/2020.03.19.20038794

Paul, S., & Venkateswaran, J. (2020). Designing robust policies under deep uncertainty for mitigating epidemics. *Computers and Industrial Engineering, 140*. https://doi.org/10.1016/j.cie.2019.106221

Prem, K., Liu, Y., Russell, T. W., Kucharski, A. J., Eggo, R. M., Davies, N., Jit, M., Klepac, P., Flasche, S., Clifford, S., Pearson, C. A. B., Munday, J. D., Abbott, S., Gibbs, H., Rosello, A., Quilty, B. J., Jombart, T., Sun, F., Diamond, C., … Hellewell, J. (2020). The effect of control strategies that reduce social mixing on outcomes of the

COVID-19 epidemic in Wuhan, China. *MedRxiv*. https://doi.org/10.1101/2020.03.09.20033050

Read, J. M., Bridgen, J. R. E., Cummings, D. A. T., Ho, A., & Jewell, C. P. (2020). Novel coronavirus 2019-nCoV: Early estimation of epidemiological parameters and epidemic predictions. *MedRxiv*. https://doi.org/10.1101/2020.01.23.20018549

Tang, B., Bragazzi, N. L., Li, Q., Tang, S., Xiao, Y., & Wu, J. (2020). An updated estimation of the risk of transmission of the novel coronavirus (2019-nCov). *Infectious Disease Modelling, 5*, 248–255. https://doi.org/10.1016/j.idm.2020.02.001

Tang, B., Wang, X., Li, Q., Bragazzi, N. L., Tang, S., Xiao, Y., & Wu, J. (2020). Estimation of the transmission risk of the 2019-nCoV and its implication for public health interventions. *Journal of Clinical Medicine, 9*(2), Article 462. https://doi.org/10.3390/jcm9020462

Verity, R., Okell, L. C., Dorigatti, I., Winskill, P., Whittaker, C., Imai, N., Cuomo-Dannenburg, G., Thompson, H., Walker, P. G. T., Fu, H., Dighe, A., Griffin, J. T., Baguelin, M., Bhatia, S., Boonyasiri, A., Cori, A., Cucunubá, Z., FitzJohn, R., Gaythorpe, K., … Ferguson, N. M. (2020). Estimates of the severity of coronavirus disease 2019: A model-based analysis. *The Lancet Infectious Diseases, 20*(6), 669–677. https://doi.org/10.1016/S1473-3099(20)30243-7

Wang, J. Z., & Peng, W. H. (2020). Fluctuations for the outbreak prevalence of the SIR epidemics in complex networks. *Physica A: Statistical Mechanics and Its Applications, 548*, Article 123848. https://doi.org/10.1016/j.physa.2019.123848

Wang, X., Tang, S., Chen, Y., Feng, X., Xiao, Y., & Xu, Z. (2020). When will be the resumption of work in Wuhan and its surrounding areas during COVID-19 epidemic? A data-driven network modeling analysis. *Scientia Sinica Mathematica, 50*(7), 969–978. https://doi.org/10.1360/SSM-2020-0037

Weeden, K., & Cornwell, B. (2020). The small-world network of college classes: Implications for epidemic spread on a university campus. *Sociological Science, 7*, 222–241. https://doi.org/10.15195/v7.a9

Zeng, T., Zhang, Y., Li, Z., Liu, X., & Qiu, B. (2020). Predictions of 2019-nCoV transmission ending via comprehensive methods. *ArXiv*. https://arxiv.org/abs/2002.04945.

Zhang, C., Qian, L. X., & Hu, J. Q. (2020). Pathways of the COVID-19 pandemic with human mobility across countries. *MedRxiv*. https://doi.org/10.1101/2020.05.21.20108589

Zhu, G., Chen, G., Zhang, H., & Fu, X. (2015). Propagation dynamics of an epidemic model with infective media connecting two separated networks of populations. *Communications in Nonlinear Science and Numerical Simulation, 20*(1), 240–249. https://doi.org/10.1016/j.cnsns.2014.04.023

Zhu, G., Fu, X., & Chen, G. (2012). Spreading dynamics and global stability of a generalized epidemic model on complex heterogeneous networks. *Applied Mathematical Modelling, 36*(12), 5808–5817. https://doi.org/10.1016/j.apm.2012.01.023